Resistive Switching Memory Based on Bioinspired Natural Solid Polymer Electrolytes

ARTICLE *in* ACS NANO · DECEMBER 2014

Impact Factor: 12.88 · DOI: 10.1021/nn5055909

Resistive Switching Memory Based on Bioinspired Natural Solid Polymer Electrolytes

Niloufar Raeis Hosseini and Jang-Sik Lee*

Department of Materials Science and Engineering, Pohang University of Science and Technology (POSTECH), Pohang 790-784, South Korea

ABSTRACT A solution-processed, chitosan-based resistive-switching memory device is demonstrated with Pt/Ag-doped chitosan/Ag structure. The memory device shows reproducible and reliable bipolar resistive switching characteristics. A memory device based on natural organic material is a promising device toward the next generation of nonvolatile nanoelectronics. The memory device based on chitosan as a natural solid polymer electrolyte can be switched reproducibly between high and low resistance states. In addition, the data retention measurement confirmed the reliability of the chitosan-based nonvolatile memory device. The transparent Ag-embedded chitosan film showed an acceptable and comparable resistive switching behavior on the flexible plastic substrate as well. A cost-effective, environmentally benign memory device using chitosan satisfies the functional requirements of nonvolatile memory operations.

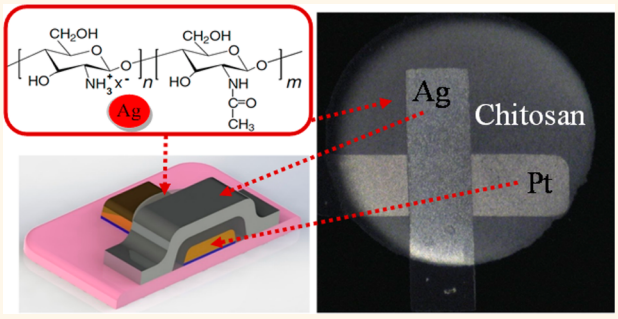

KEYWORDS: chitosan · natural solid polymers · redox-based memory · solution processes · resistive switching memory

Redox-based resistive switching memories (ReRAMs) for next-generation nanoelectronics offer exceptional prospects, for example, fast response time,[1−4] multilevel data storage,[1,5] high density,[1,6−8] low power consumption,[2−4,8] nonvolatility,[6] high performance,[4,6,8] and good reliability.[1,9] A wide range of materials can be used such as organics,[10−12] inorganics,[13−16] and hybrid nanocomposites[17,18] as their components. ReRAMs based on organic materials are emerging nonvolatile memories with various advantages, such as flexibility,[19−21] transparency,[20,22] printability,[19,21,23] scalability,[23] compatibility with diverse substrates,[24] and processability to variable forms.[19,21,24]

Recently, various organic materials including polymers have been used in nonvolatile memory elements that have resistive switching behavior.[25−27] Among them, biomolecules show promise for use as materials for ReRAM devices because the molecules are inexpensive, environmentally benign, and biocompatible as well as flexible.[28] Consequently, natural materials are being considered as potential candidates for biocompatible electronics. However, practical application of biomolecules to the nonvolatile memory devices requires feasibility assessment. On the other hand, fabrication of biodegradable ReRAM is highly desired in view of their natural abundance, disposability, and low cost.[29−31]

Moreover, a memristor-like device based on soft materials operating on an ionic conductance mechanism has been reported. This flexible device is composed of two liquid metal electrodes and a sandwiched hydrogel as a biocompatible media with high ion mobility due to high water content.[32] To mimic the brain architecture and synaptic connections between neurons, an ionic two-terminal memory device has been introduced. The ionic (H^+) conductivity is produced among a proton conducting Nafion embedded between two PdH_x electrodes.[33]

Although a few studies have been dedicated to develop bioinspired materials to get employed in ReRAM components, there still exist areas for further development.[34−36] Solid polymer electrolytes (SPEs) can be used in cation-based electrochemical switching memories because of their simple structure

* Address correspondence to jangsik@postech.ac.kr.

Received for review October 1, 2014 and accepted December 11, 2014.

Published online 10.1021/nn5055909

and facile operation.[27] When subjected to an electric field, SPEs behave as liquid electrolytes as a result of electrochemical reactions and ion migration. Electrochemical metal accumulation and dissolution strongly affect switching phenomena on electrochemical metallization (ECM) cells. Various types of electrolytes in ECM cells can show switching characteristics because they have high ionic conductivity of corresponding cations.[8]

In this study, we used chitosan as a bioinspired SPE and applied to the resistive switching element in ReRAM. Chitosan is a cationic biopolymer derived by deacetylation of chitin with similar monomers by replacing an NH_2 functional group with $HNCOCH_3$.[37] Chitosan also contains a repeated β(1,4)-linked 2-acetoamiodo-2-deoxy-D-glucose unit of N-deacetylated chitin (Scheme S1, Supporting Information).[38] Chitosan-based bio-SPE with a polysaccharide matrix is a potential candidate for bioinspired electro-active polymer-based materials. It has a wide variety of potential applications in devices, such as biosensors, actuators, solar cells, high-capacity batteries, and fuel cells.[38,39]

This study investigates the suitability of chitosan as a resistive switching layer in ReRAMs for biocompatible electronic devices. Four characteristics suggest that its use in this application is feasible. (1) Chitosan is an insulator in its native state under ambient conditions, but its ionic conductivity can be tuned by using appropriate amounts of salts and plasticizers. Nonconducting chitosan can form an Ag^+ conductor polymer upon doping with silver nitrate.[40] (2) Amine and hydroxyl polar groups of chitosan make it soluble in diluted acid solution. Amine groups of chitosan are extremely reactive with metal ions due to free electron doublets of nitrogen atoms that uptake metal cations by a chelating mechanism.[41] (3) Chitosan has a strong ability to make uniform, stable, and transparent films with medium molecular weight, which is appropriate to produce transparent electronic devices. (4) Chitosan has been suggested as a proton conductor thin film for transistor on glass and bendable paper substrate.[42−44] Its biocompatibility and abundance in unused crab shells/mushrooms make it an inexpensive, nontoxic, and biocompatible polymer for emerging device applications.

This study introduces a novel biodegradable natural SPE material for use in developing nanostructured nonvolatile organic memory devices. We elucidate switching behavior of natural chitosan-based thin films and investigate its feasibility in application for nonvolatile resistive switching memory devices. We successfully fabricated and characterized an environmentally benign, biocompatible, and disposable ReRAM device based on chitosan. The application of chitosan in nanoelectronic devices with solution-assisted processes is therefore an inexpensive and biocompatible way to fabricate novel memory devices.

RESULTS AND DISCUSSION

A Pt (bottom electrode)/Ag-doped chitosan thin film (resistive switching layer)/Ag (top electrode) sandwiched structure (Figure 1a−c) was used to demonstrate the nonvolatile resistive switching behavior of chitosan. A 20 nm Ti adhesion layer and 100 nm Pt was deposited and patterned using a shadow mask for use as a bottom electrode (BE) on a Si/SiO_2 substrate. Afterward, an Ag-doped chitosan solution was drop-casted onto the inert BE and dried at room temperature overnight to make a resistive switching layer. Finally, a 100 nm thick Ag film as top electrode (TE) was patterned using a shadow mask by thermal evaporation to make a metal/insulator/metal (MIM) structure with a cross junction area of $100 \times 100\ \mu m^2$. The transparent polymer electrolyte was well-casted on the device (Figure 1c).

The chitosan-based ReRAM showed typical resistive switching behavior (Figure 2 a). Current−voltage (I−V) responses of the Pt/Ag-doped chitosan/Ag device were measured under dc sweeping voltage applied as 0 V → 1.5 V → 0 V → −1.5 V → 0 V to the TE (Ag); the BE (Pt) was grounded (Figure 2 a; inset). Both low resistance state (LRS) and high-resistance state (HRS) were observed. During the first voltage sweep (upon applying the positive bias) from zero to set voltage ($V_{set} \sim 0.5$ V), Ag in the top electrode dissolved and oxidized to Ag^+, and the cations started to form a conductive filament (CF) at the interface of the Pt counter-electrode by reducing to Ag atoms. After the CF was formed, the insulating chitosan-based SPE was assumed to be the LRS. A compliance current of 0.1 mA was used to prevent device breakdown. Conversely, applying a voltage of opposite polarity ruptured the CF and switched the device back to the HRS.

A data retention test was performed to appraise the memory performance of the Pt/Ag-doped chitosan/Ag device. Data retention characterization for both of the ON and OFF states were executed with a reading bias of 0.2 V under ambient conditions. A high ON/OFF ratio of $\sim 10^5$ was achieved in the chitosan-based ReRAM device, and no discernible degradation in the current of LRS and HRS was observed over 10^4 s (Figure 2b). To evaluate the endurance property, a repeated cyclic test was performed. We measured up to 100 cycles and found almost no change in electrical property (Supporting Information, Figure S1). This indicates the robust programmable memory property of chitosan-based memory cells. These results demonstrate that this memory device satisfies the functional demands of nonvolatile memory.

We also examined the resistive switching behavior of undoped-chitosan as SPE in the aforementioned structure by applying a voltage up to 10 V to the TE (Ag) while grounding BE (Pt) (Figure 3 a). The device was formed at 6 V. The voltage was swept as 0 V → 3 V → 0 V → −3 V → 0 V (Figure 3b). As a comparison, the Ag-doped

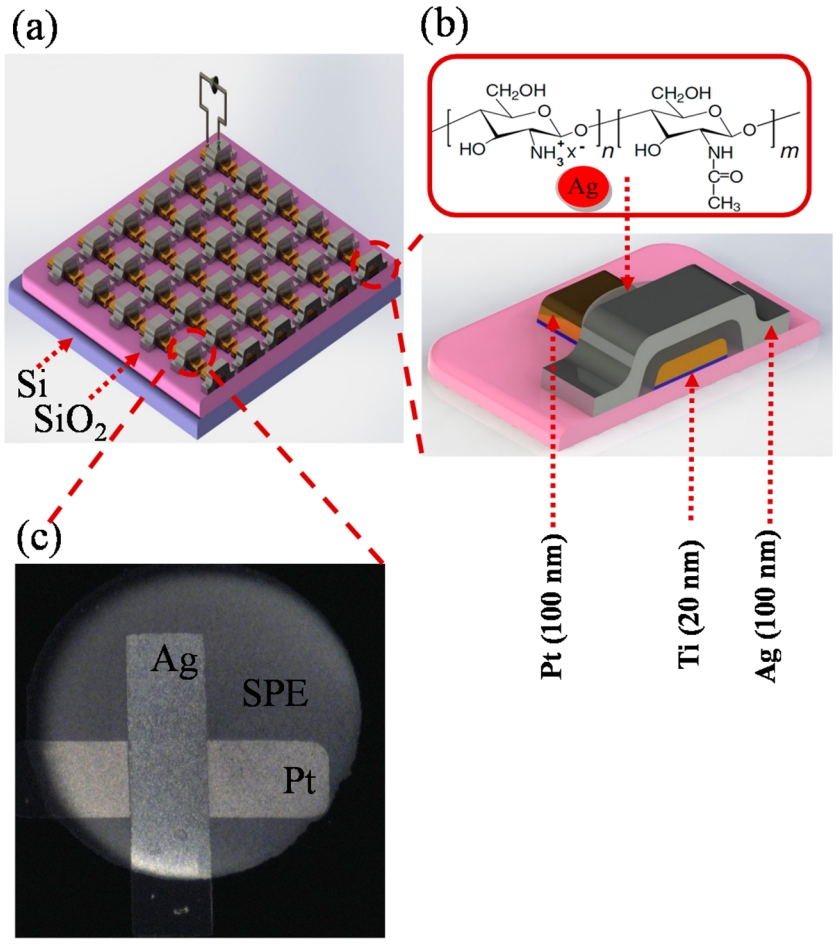

Figure 1. (a) Schematic illustration of device architectures, (b) a unit device configuration with Ag-doped chitosan as resistive switching layer, and (c) optical image of cross junction electrodes with drop-casted chitosan solid polymer eletrolyte.

devices did not need any forming voltage to get LRS, and they worked better at lower voltages than undoped devices.

In undoped chitosan there is a fluctuation in switching V_{set} due to the random nature of CF and its instability. The variation of the set process in undoped chitosan film may come from the variation of the number and/or the size of CF (Figure 3b). The variation in V_{set} was solved by Ag doping in the chitosan layer, which suppresses the random formation of CF (Figure 2a). The presence of Ag ions in the chitosan layer makes preferential paths of CF and supports the uniform filament, which effectively reduces the fluctuation in the set part. Furthermore, formation and rupture of the CF is more stabilized through Ag doping in the chitosan layer. The variation in the reset process is thought to be related to dissociation of the CF in random locations. It is found that V_{set}, V_{reset}, HRS, and LRS are more uniform when chitosan is doped with Ag (Figure 2a).

The electrochemical properties of the Ag-doped chitosan were characterized by cyclic voltammetry (CV). A typical CV of the polymer electrolyte was investigated with a Pt working electrode and an Ag/Ag^+ reference electrode at a scan rate of 50 $mV \cdot s^{-1}$. The current responses were recorded while the voltage was swept as 0 V → 0.8 V → 0 V → −0.8 V → 0 V for 5 wt % Ag embedded in chitosan solution (Figure S2, Supporting Information). The first current peak at ~0.4 V is observed due to silver incorporation into the SPE, while the sharp peak was not observed in the following scans. It is postulated to the elevated charging current by Ag^+ ions in the SPE to charge the electrical double layer. The peak appeared because of the redox process in the chitosan chains by charging the electrical double layer with Ag^+ ions in the SPE. Through the subsequent negative voltage sweep, the Ag^+ ions were reduced and a negative current occurred due to the limited diffusion of the cations into the SPE. The current peak at −0.48 V corresponded to a faradaic current because of reduction of Ag^+ and their diffusion to the top electrode among the SPE.[45] In conclusion, the rate-limiting process occurred at ~0.4 V and −0.48 V, which are indicated as silver oxidation and reduction on the Pt working electrode, respectively.[27]

On the basis of the preliminary experiments, the switching behavior of chitosan film is ascribed to the dispersion of ions and to their interaction with SPE.

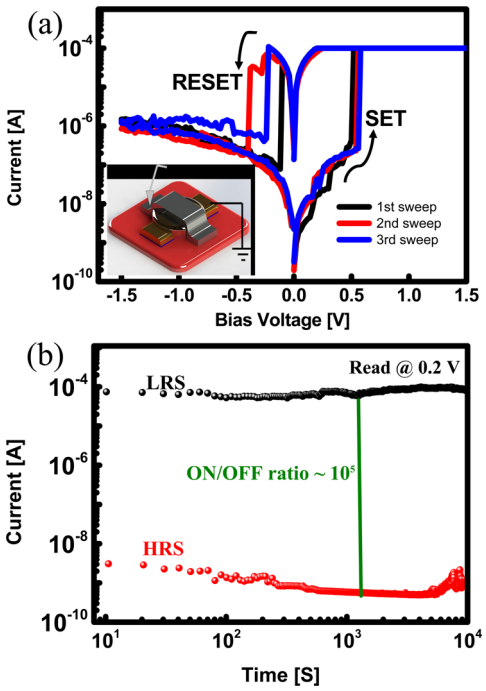

Figure 2. (a) Semilogarithmic I–V characteristics of the chitosan-based resistive switching memory device with an $AgNO_3$ concentration of 5 wt % at ambient temperature; inset: illustration of a unit device configuration to measure the electrical properties. (b) Data retention characteristics of LRS and HRS states under continuous readout voltage at room temperature.

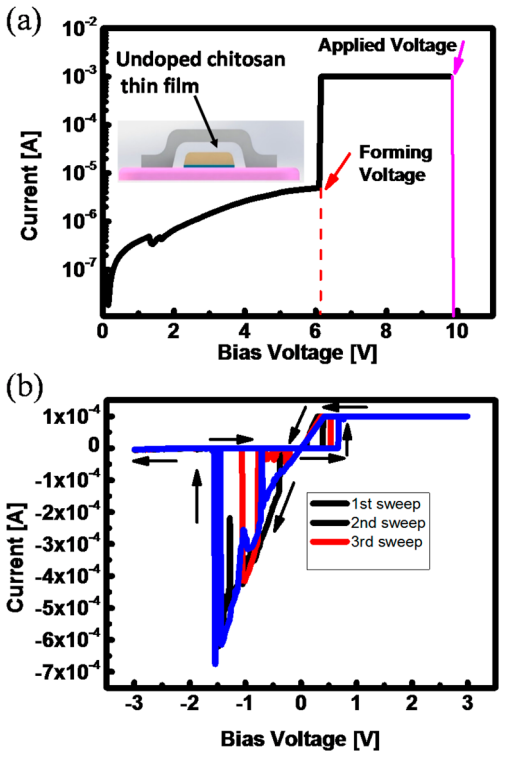

Figure 3. (a) Forming process to initiate the resistive switching of undoped chitosan-based resistive switching memory. Inset: the schematic cross-sectional view of chitosan-based MIM structure. (b) Typical I–V curve of Pt/undoped chitosan/Ag memory device with a 10^{-4} A current compliance; the sweep direction is indicated by arrows.

The reactive groups (OH^- and NH_2) may interact with Ag^+ by two distinct mechanisms depending on pH and on the nature of the solution matrix.[41] In fact, pH affects chelation and electrochemical attraction that are responsible for attachment and detachment of Ag^+ and NO_3^- to chitosan. As the pH decreases, protonation of NH_2 increases and causes repulsion of metal cations. Chelation of cations by ligands in the chitosan solution causes creation of metal anions;[46] subsequently the chelation process is changed to electrostatic attraction of protonated amine groups. In addition, a high ionic conductivity of hydrated chitosan films is attributed to the hydroxyl ions. Amine sites may be the most important reactive group for metal ions, whereas hydroxyl groups are conducive to sorption.[47] Electrostatic attraction between NO_3^- and protonated amine groups occurs in acetic acid solution.[41] Because some of the amine sites form intermolecular hydrogen bonds, the accessible free amine groups contribute to absorption of Ag^+.[48] In a weakly acidic solution, Ag^+ ions bind with free electron pairs on nitrogen. Cationic behavior of chitosan is achieved by protonation of amine groups in acetic acid solution and pH adjustment, which leads to attraction of NO_3^- to its chain (Scheme S2a–d, Supporting Information). The reaction direction of chelation is sensitive to pH.[48,49] The color of the chitosan solution changed from colorless to gray blue after addition of silver nitrate upon stirring. We postulate this phenomenon is caused by the bounding of Ag^+ ions in the polysaccharide template *via* electrostatic collaborations like ion–dipole interactions.

To confirm the aforementioned reaction, UV–vis absorption spectra was recorded for both of undoped chitosan and an Ag doped chitosan solutions (Figure S3, Supporting Information). $AgNO_3$ solution was selected as a reference material to check the absorbance of the Ag-embedded chitosan, and it showed two peaks at 214 and 300 nm. The chitosan acetate solution had a minor peak around 300 nm, while the mixture of chitosan and $AgNO_3$ denotes a representative peaks at 236 nm with a small peak at 300 nm. The high absorbance peak at 200 and 236 nm indicates the increased amount of Ag in the chitosan solution because chitosan makes a complex with Ag cations as a polymeric chelating agent using its amino groups.[50] Additionally the electropositive Ag^+ cations are believed to interact with the electron-rich oxygen atoms of polar hydroxyl group and the remaining ether groups in chitosan.[51]

The inferred switching mechanism of the Pt/Ag-doped chitosan/Ag device is formation and rupture of conducting filament (Figure 4a–d). During application of proper positive bias voltage to the TE of the pristine device, Ag^+ cations migrate toward the BE (Pt) and NO_3^- anions move to the TE (Ag). Oxidation

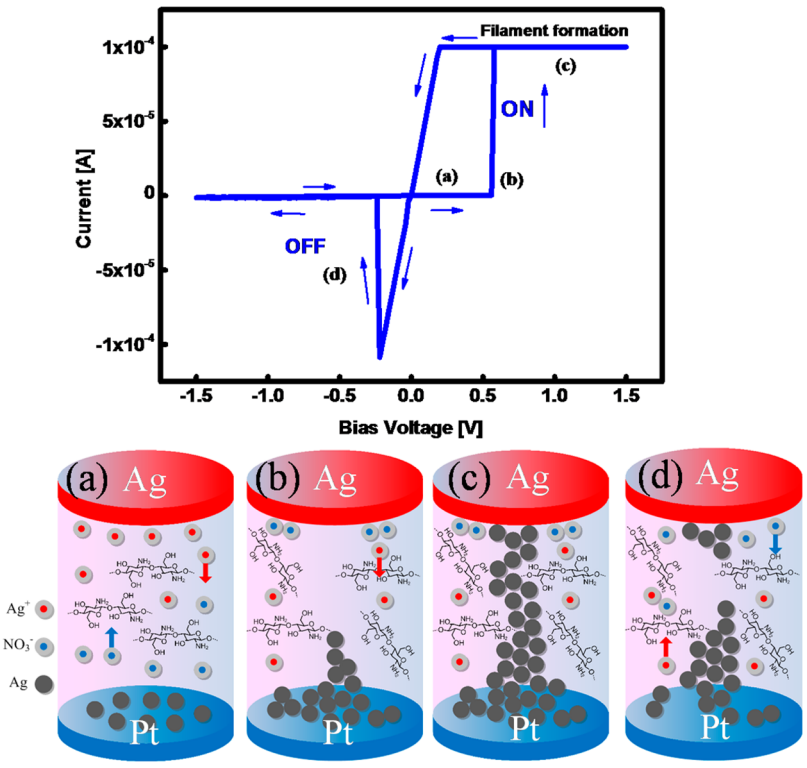

Figure 4. Proposed resistive switching mechanism of Pt/Ag-doped chitosan SPE/Ag device with linear I−V characteristics of the resistive switching memory device: (a) Ag^+ and NO_3^- ion movement under positive bias voltage; (b) beginning of Ag filament formation (nucleation of filament); (c) connection of two electrodes *via* conductive filament (CF); (d) rupture of filament under negative bias.

(anodic dissolution) occurs at the interface of Ag and SPE ($Ag \rightarrow Ag^+ + e^-$) because the TE behaves as the anode of an electrochemical cell. Ordinarily, under a high electric field, Ag^+ cations drift across the SPE thin film and travel toward the BE under positive bias (Figure 4 a). In contrast, the BE is responsible for the cathodic deposition reaction, and Ag^+ ions at the SPE and BE interface are reduced to nonionic Ag atoms ($Ag^+ + e^- \rightarrow Ag$). Accordingly, neutral Ag atoms are electrodeposited on the BE surface.

It has been proven that the electric field induces electrochemical deposition of Ag.[52] Meanwhile already-deposited Ag atoms self-assemble into Ag filaments to the TE (Figure 4b) and thereby create a conductive route between TE and BE (Figure 4c). This phenomenon is equivalent to a short circuit in electrochemical cells; hence, we call it the ON state. In our system, we adjusted current compliance to ~0.1 mA to avoid device breakdown. Thus, after filament formation, the conducted voltage decreases because of current compliance to prevent additional Ag deposition and protects the device from permanent collapse. To switch the device to its virgin state, we applied a sufficient opposite voltage to rupture the filament ($Ag \rightarrow Ag^+ + e^-$), while Ag^+ cations move toward the TE to get reduced to Ag atoms and make an initial HRS state ($Ag^+ + e^- \rightarrow Ag$). In conclusion, the filament annihilation occurs by subsequent negative voltage, which leads to discontinuity in the narrow part of the CF. The faradaic current in parallel with an electronic current in CF leads to dissolution of the filament[52] (Figure 4d). Our device showed reproducible resistive switching behavior by adequate application of electrical biases. Repetitive cyclic operations were achieved in the memory device using Ag-doped chitosan SPE, which is postulated to result from formation and dissolution of Ag filaments.

For real device application, it is very important to fabricate high-density memory devices. Multilevel data storage is used to utilize the different data levels in a unit memory device. Therefore, it can increase the memory density without device size reduction. The set part was controlled by applying different current compliances, while the reset process was accomplished during negative bias sweep. Four different data levels were obtained (Figure S4, Supporting Information). Further optimization of multilevel data storage will be done by extending the study shown here.

On the other hand, flexible and transparent electronic devices are highly desired for the next generation of flexible nanoelectronics to their application in wearable electronics.[36] Therefore, we demonstrated the fabrication of flexible resistive switching memory device with an Ag-doped chitosan as the switching layer. The Pt/SPE/Ag structure was fabricated on flexible poly(ether sulfone) (PES) plastic substrates (Figure 5a).

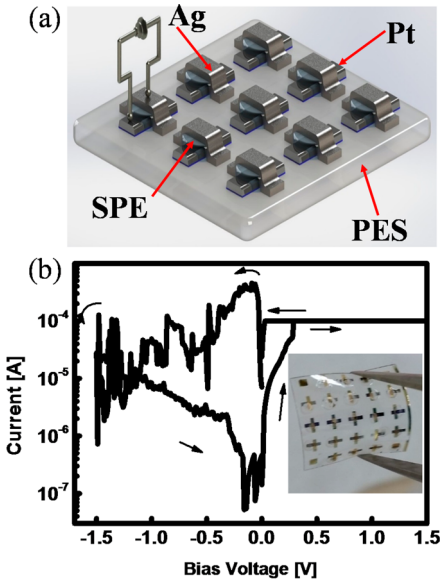

Figure 5. (a) Schematic illustration of flexible memory device with Pt/Ag-doped chitosan SPE/Ag resistive switching memory fabricated on flexible plastic substrate. (b) Resistive switching behavior of the flexible memory device with a current compliance of 10^{-4} A; inset: optical image of chitosan-based memory devices fabricated on the flexible substrate.

The device fabrication method was the same as for devices fabricated on silicon substrates. The flexible chitosan-based ReRAM device was successfully fabricated with resistive switching behavior (Figure 5b). In addition, the data retention property of the flexible devices showed almost no loss of memory performance with time (Figure S5, Supporting Information). It is confirmed that the chitosan device has good potential to be applied for nanostructured transparent and flexible memory devices. Further experiments to confirm the nonvolatility of the mentioned device are currently under the way. Upon optimization of chitosan-based ReRAM device, such natural and disposable material would be a beneficial candidate for emerging flexible memory applications.

CONCLUSIONS

Ag-doped chitosan is introduced as the biocompatible resistive switching layer of ReRAM. We fabricated ReRAM based on chitosan that can be operated with low power consumption. It is a promising candidate for both environmentally friendly and inexpensive memory devices. We demonstrate the resistive switching characteristics of Ag-doped chitosan with bipolar switching properties for nonvolatile memory applications. Reproducible and reliable bipolar resistive switching behavior was obtained. Furthermore, the fabricated device showed a noteworthy memory performance with a high on−off ratio ($\sim 10^5$) and reasonable data retention time ($\sim 10^4$ s). Based on electrical measurement, we suggest that the formation and rupture of metallic silver filaments by electrochemical reactions are responsible for the observed bipolar resistive switching behavior. This study demonstrates that memory devices based on bioinspired materials can facilitate fabrication of biocompatible and flexible ReRAMs. The chitosan-based device is extremely inexpensive because it can be fabricated from biological waste products such as crab shells.

METHODS

Materials and Device Fabrication. The ReRAM devices were fabricated with a Pt/SPE/Ag structure on both silicon and flexible substrates, respectively. For the former, the thermally oxidized silicon (SiO_2, thickness of 100 nm) substrates were treated with piranha solution and cleaned using acetone, ethanol, 2-propanol, and distilled water following sonication for 10 min and then dried using N_2 gas. For the latter, PES was used as the flexible substrate. The PES substrates were ultrasonically cleaned using ethanol, 2-propanol, and distilled water for 5 min.

A 20 nm Ti adhesion layer and a 100 nm Pt electrode were deposited on the substrate by E-beam evaporation and sputtering, respectively. Crab shell-based chitosan with a medium molecular weight (deacetylation degree 75−85%, Sigma-Aldrich) was dissolved (0.5 wt/v %) in 1% acetic acid solution in distilled water, mixed overnight under ambient temperature and constant stirring at 120 rpm, and then filtered through a syringe filter. $AgNO_3$ powder (99.9999%, Sigma-Aldrich) was mixed with the chitosan solution at 1, 3, 5, 6, and 9 wt %. On the basis of empirical electrical characteristics, the 5 wt % Ag to chitosan solution was selected as the best concentration ratio for use in the rest of the experiments. (We characterized the electrical properties by measuring the current of each device with applied voltage and found that the resistive switching behaviors were dependent on the concentration of the doped $AgNO_3$. If Ag concentration is lower (<5 wt %) the devices are set at high voltages. If Ag concentration is higher (>5 wt %) the memory window is not wide enough (low ON/OFF ratio), and a breakdown occurs at 9 wt %, so we conclude that for Ag-doped layers more than 5 wt % the devices have a tendency to show almost metallic behavior. From these electrical characterizations we found that 5% Ag doping is best concentration in terms of memory performance.)

The 0.5 wt % diluted chitosan acetate solution was doped with Ag cations then drop-casted on the patterned Pt BE. The Ag-doped chitosan film was dried at ambient temperature overnight then vacuum annealed at 60 °C for 6 h to get a uniform layer. The Ag top electrode was deposited using thermal evaporation and patterned to make a cross-junction ReRAM device.

Characterization. UV−vis spectra were performed with an Agilent Cary 100 UV−vis spectrophotometer operating in the absorption mode. The redox properties of the polymer electrolyte were measured using a potentiostat (Gamry instruments, Reference 3000, USA). Electrical characteristics of the fabricated devices were conducted at atmospheric pressure under ambient temperature using a semiconductor parameter analyzer (Keithley 4200-SCS, USA) for applying voltages and measuring currents. In a typical test configuration, the sample was placed in a probe station, and bias voltages were applied to the Ag top electrode while the Pt bottom electrode was grounded. The current−voltage (I−V) measurements were performed with forward and backward voltage sweeps.

Conflict of Interest: The authors declare no competing financial interest.

Supporting Information Available: Schematic formula of chitin, chitosan, UV−vis absorption spectra, endurance behavior, electrochemical CV of SPE, multilevel data storage capability, and data retention for flexible memory device in Schemes S1 and S2 and Figures S1−S5. This material is available free of charge *via* the Internet at http://pubs.acs.org.

Acknowledgment. This work was supported by the National Research Foundation (NRF) grant funded by the Korea government (MEST) (2010-0015014) and by the Future Semiconductor Device Technology Development Program (10045226) funded by the Ministry of Trade, Industry & Energy (MOTIE) and Korea Semiconductor Research Consortium (KSRC). In addition, this work was partially supported by Brain Korea 21 PLUS project (Center for Creative Industrial Materials).

REFERENCES AND NOTES

1. Lu, W.; Jeong, D. S.; Kozicki, M.; Waser, R. Electrochemical Metallization Cells—Blending Nanoionics into Nanoelectronics? *MRS Bull.* **2012**, *37*, 124–130.
2. Tappertzhofen, S.; Valov, I.; Tsuruoka, T.; Hasegawa, T.; Waser, R.; Aono, M. Generic Relevance of Counter Charges for Cation-Based Nanoscale Resistive Switching Memories. *ACS Nano* **2013**, *7*, 6396–6402.
3. Valov, I.; Linn, E.; Tappertzhofen, S.; Schmelzer, S.; van den Hurk, J.; Lentz, F.; Waser, R. Nanobatteries in Redox-Based Resistive Switches Require Extension of Memristor Theory. *Nat. Commun.* **2013**, *4*, 1771.
4. Yang, J. J.; Strukov, D. B.; Stewart, D. R. Memristive Devices for Computing. *Nat. Nanotechnol.* **2013**, *8*, 13–24.
5. Qi, J.; Olmedo, M.; Zheng, J.-G.; Liu, J. Multimode Resistive Switching in Single ZnO Nanoisland System. *Sci. Rep.* **2013**, *3*, 2405.
6. Linn, E.; Rosezin, R.; Kügeler, C.; Waser, R. Complementary Resistive Switches for Passive Nanocrossbar Memories. *Nat. Mater.* **2010**, *9*, 403–406.
7. Waser, R.; Aono, M. Nanoionics-Based Resistive Switching Memories. *Nat. Mater.* **2007**, *6*, 833–840.
8. Waser, R.; Dittmann, R.; Staikov, G.; Szot, K. Redox-Based Resistive Switching Memories - Nanoionic Mechanisms, Prospects, and Challenges. *Adv. Mater.* **2009**, *21*, 2632–2663.
9. Oligschlaeger, R.; Waser, R.; Meyer, R.; Karthäuser, S.; Dittmann, R. Resistive Switching and Data Reliability of Epitaxial (Ba,Sr)TiO_3 Thin Films. *Appl. Phys. Lett.* **2006**, *88*, 042901.
10. Cho, B.; Yun, J. M.; Song, S.; Ji, Y.; Kim, D. Y.; Lee, T. Direct Observation of Ag Filamentary Paths in Organic Resistive Memory Devices. *Adv. Funct. Mater.* **2011**, *21*, 3976–3981.
11. Kuegeler, C.; Meier, M.; Rosezin, R.; Gilles, S.; Waser, R. High Density 3D Memory Architecture Based on the Resistive Switching Effect. *Solid-State Electron.* **2009**, *53*, 1287–1292.
12. Gao, S.; Song, C.; Chen, C.; Zeng, F.; Pan, F. Dynamic Processes of Resistive Switching in Metallic Filament-Based Organic Memory Devices. *J. Phys. Chem. C* **2012**, *116*, 17955–17959.
13. Akinaga, H.; Shima, H. Resistive Random Access Memory (ReRAM) Based on Metal Oxides. *Proc. IEEE* **2010**, *98*, 2237–2251.
14. Sawa, A. Resistive Switching in Transition Metal Oxides. *Mater. Today* **2008**, *11*, 28–36.
15. Szot, K.; Speier, W.; Bihlmayer, G.; Waser, R. Switching the Electrical Resistance of Individual Dislocations in Single-Crystalline $SrTiO_3$. *Nat. Mater.* **2006**, *5*, 312–320.
16. Tsuruoka, T.; Terabe, K.; Hasegawa, T.; Aono, M. Forming and Switching Mechanisms of a Cation-Migration-Based Oxide Resistive Memory. *Nanotechnology* **2010**, *21*, 425205.
17. Jo, S. H.; Kim, K.-H.; Lu, W. Programmable Resistance Switching in Nanoscale Two-Terminal Devices. *Nano Lett.* **2008**, *9*, 496–500.
18. Kim, T. W.; Yang, Y.; Li, F.; Kwan, W. L. Electrical Memory Devices Based on Inorganic/Organic Nanocomposites. *NPG Asia Mater.* **2012**, *4*, e18.
19. Ji, Y.; Cho, B.; Song, S.; Kim, T. W.; Choe, M.; Kahng, Y. H.; Lee, T. Stable Switching Characteristics of Organic Nonvolatile Memory on a Bent Flexible Substrate. *Adv. Mater.* **2010**, *22*, 3071–3075.
20. Kim, H.-D.; Yun, M. J.; Lee, J. H.; Kim, K. H.; Kim, T. G. Transparent Multi-Level Resistive Switching Phenomena Observed in ITO/RGO/ITO Memory Cells by the Sol-Gel Dip-Coating Method. *Sci. Rep.* **2014**, *4*, 4614.
21. Lee, T.; Chen, Y. Organic Resistive Nonvolatile Memory Materials. *MRS Bull.* **2012**, *37*, 144–149.
22. Yao, J.; Lin, J.; Dai, Y.; Ruan, G.; Yan, Z.; Li, L.; Zhong, L.; Natelson, D.; Tour, J. M. Highly Transparent Nonvolatile Resistive Memory Devices from Silicon Oxide and Graphene. *Nat. Commun.* **2012**, *3*, 1101.
23. Kim, J. J.; Cho, B.; Kim, K. S.; Lee, T.; Jung, G. Y. Electrical Characterization of Unipolar Organic Resistive Memory Devices Scaled Down by a Direct Metal-Transfer Method. *Adv. Mater.* **2011**, *23*, 2104–2107.
24. Ji, Y.; Zeigler, D. F.; Lee, D. S.; Choi, H.; Jen, A. K.-Y.; Ko, H. C.; Kim, T.-W. Flexible and Twistable Non-Volatile Memory Cell Array with All-Organic One Diode−One Resistor Architecture. *Nat. Commun.* **2013**, *4*, 2707.
25. Lin, W. P.; Liu, S. J.; Gong, T.; Zhao, Q.; Huang, W. Polymer-Based Resistive Memory Materials and Devices. *Adv. Mater.* **2014**, *26*, 570–606.
26. Song, S.; Cho, B.; Kim, T. W.; Ji, Y.; Jo, M.; Wang, G.; Choe, M.; Kahng, Y. H.; Hwang, H.; Lee, T. Three-Dimensional Integration of Organic Resistive Memory Devices. *Adv. Mater.* **2010**, *22*, 5048–5052.
27. Wu, S.; Tsuruoka, T.; Terabe, K.; Hasegawa, T.; Hill, J. P.; Ariga, K.; Aono, M. A Polymer-Electrolyte-Based Atomic Switch. *Adv. Funct. Mater.* **2011**, *21*, 93–99.
28. Irimia-Vladu, M.; Głowacki, E. D.; Voss, G.; Bauer, S.; Sariciftci, N. S. Green and Biodegradable Electronics. *Mater. Today* **2012**, *15*, 340–346.
29. Hota, M. K.; Bera, M. K.; Kundu, B.; Kundu, S. C.; Maiti, C. K. A Natural Silk Fibroin Protein-Based Transparent Bio-Memristor. *Adv. Funct. Mater.* **2012**, *22*, 4493–4499.
30. Hung, Y.-C.; Hsu, W.-T.; Lin, T.-Y.; Fruk, L. Photoinduced Write-Once Read-Many-Times Memory Device Based on DNA Biopolymer Nanocomposite. *Appl. Phys. Lett.* **2011**, *99*, 253301.
31. Meng, F.; Jiang, L.; Zheng, K.; Goh, C. F.; Lim, S.; Hng, H. H.; Ma, J.; Boey, F.; Chen, X. Protein-Based Memristive Nanodevices. *Small* **2011**, *7*, 3016–3020.
32. Koo, H.-J.; So, J.-H.; Dickey, M. D.; Velev, O. D. Towards All-Soft Matter Circuits: Prototypes of Quasi-Liquid Devices with Memristor Characteristics. *Adv. Mater.* **2011**, *23*, 3559–3564.
33. Josberger, E. E.; Deng, Y.; Sun, W.; Kautz, R.; Rolandi, M. Two-Terminal Protonic Devices with Synaptic-Like Short-Term Depression and Device Memory. *Adv. Mater.* **2014**, *26*, 4986–4990.
34. Gogurla, N.; Mondal, S. P.; Sinha, A. K.; Katiyar, A. K.; Banerjee, W.; Kundu, S. C.; Ray, S. K. Transparent and Flexible Resistive Switching Memory Devices with a Very High On/Off Ratio Using Gold Nanoparticles Embedded in a Silk Protein Matrix. *Nanotechnology* **2013**, *24*, 345202.
35. Wang, H.; Meng, F.; Cai, Y.; Zheng, L.; Li, Y.; Liu, Y.; Jiang, Y.; Wang, X.; Chen, X. Sericin for Resistance Switching Device with Multilevel Nonvolatile Memory. *Adv. Mater.* **2013**, *25*, 5498–5503.
36. Nagashima, K.; Koga, H.; Celano, U.; Zhuge, F.; Kanai, M.; Rahong, S.; Meng, G.; He, Y.; De Boeck, J.; Jurczak, M.; *et al.* Cellulose Nanofiber Paper as an Ultra Flexible Nonvolatile Memory. *Sci. Rep.* **2014**, *4*, 5532.
37. Zhong, C.; Deng, Y.; Roudsari, A. F.; Kapetanovic, A.; Anantram, M.; Rolandi, M. A Polysaccharide Bioprotonic Field-Effect Transistor. *Nat. Commun.* **2011**, *2*, 476.
38. Finkenstadt, V. L. Natural Polysaccharides as Electroactive Polymers. *Appl. Microbiol. Biotechnol.* **2005**, *67*, 735–745.
39. Wan, Y.; Peppley, B.; Creber, K. A. M.; Bui, V. T.; Halliop, E. Preliminary Evaluation of an Alkaline Chitosan-Based Membrane Fuel Cell. *J. Power Sources* **2006**, *162*, 105–113.

40. Morni, N.; Mohamed, N.; Arof, A. Silver Nitrate Doped Chitosan Acetate Films and Electrochemical Cell Performance. *Mater. Sci. Eng., B* **1997**, *45*, 140–146.
41. Guibal, E. Interactions of Metal Ions with Chitosan-Based Sorbents: A Review. *Sep. Purif. Technol.* **2004**, *38*, 43–74.
42. Jiang, J.; Sun, J.; Dou, W.; Wan, Q. Junctionless Flexible Oxide-Based Thin-Film Transistors on Paper Substrates. *IEEE Electron Device Lett.* **2012**, *33*, 65–67.
43. Jiang, J.; Wan, Q.; Zhang, Q. Transparent Junctionless Electric-Double-Layer Transistors Gated by a Reinforced Chitosan-Based Biopolymer Electrolyte. *IEEE Trans. Electron Devices* **2013**, *60*, 1951–1957.
44. Zhou, B.; Sun, J.; Han, X.; Jiang, J.; Wan, Q. Low-Voltage Organic/Inorganic Hybrid Transparent Thin-Film Transistors Gated by Chitosan-Based Proton Conductors. *IEEE Electron Device Lett.* **2011**, *32*, 1549–1551.
45. Schindler, C.; Valov, I.; Waser, R. Faradaic Currents During Electroforming of Resistively Switching Ag−Ge−Se Type Electrochemical Metallization Memory Cells. *Phys. Chem. Chem. Phys.* **2009**, *11*, 5974–5979.
46. Wu, L.-Q.; Gadre, A. P.; Yi, H.; Kastantin, M. J.; Rubloff, G. W.; Bentley, W. E.; Payne, G. F.; Ghodssi, R. Voltage-Dependent Assembly of the Polysaccharide Chitosan onto an Electrode Surface. *Langmuir* **2002**, *18*, 8620–8625.
47. Huang, H.; Yang, X. Chitosan Mediated Assembly of Gold Nanoparticles Multilayer. *Colloids Surf., A: Physicochem. Eng. Aspects* **2003**, *226*, 77–86.
48. Murugadoss, A.; Chattopadhyay, A. A "Green" Chitosan−Silver Nanoparticle Composite as a Heterogeneous as Well as Micro-Heterogeneous Catalyst. *Nanotechnology* **2008**, *19*, 015603.
49. Tang, D.-L.; Song, F.; Chen, C.; Wang, X.-L.; Wang, Y.-Z. A Ph-Responsive Chitosan-B-Poly (P-Dioxanone) Nanocarrier: Formation and Efficient Antitumor Drug Delivery. *Nanotechnology* **2013**, *24*, 145101.
50. Wei, D.; Sun, W.; Qian, W.; Ye, Y.; Ma, X. The Synthesis of Chitosan-Based Silver Nanoparticles and Their Antibacterial Activity. *Carbohydr. Res.* **2009**, *344*, 2375–2382.
51. Huang, H.; Yuan, Q.; Yang, X. Preparation and Characterization of Metal−Chitosan Nanocomposites. *Colloid Surf., B: Biointerfaces* **2004**, *39*, 31–37.
52. Valov, I.; Waser, R.; Jameson, J. R.; Kozicki, M. N. Electrochemical Metallization Memories—Fundamentals, Applications, Prospects. *Nanotechnology* **2011**, *22*, 254003.